

SPATIALLY RESOLVED CIRCUMNUCLEAR DUST IN CENTAURUS A

MARGARITA KAROVSKA, MASSIMO MARENGO, MARTIN ELVIS, GIOVANNI G. FAZIO, AND JOSEPH L. HORA
Harvard-Smithsonian Center for Astrophysics, 60 Garden Street, Cambridge, MA 02138; karovska@cfa.harvard.edu

AND

PHILIP M. HINZ, WILLIAM F. HOFFMANN, MICHAEL MEYER, AND ERIC MAMAJEK
Steward Observatory, University of Arizona, 933 North Cherry Avenue, Tucson, AZ 85721-0065

Received 2003 August 5; accepted 2003 October 17; published 2003 November 12

ABSTRACT

In this Letter, we present results from our exploratory mid-IR study of Centaurus A circumnuclear environment using high angular resolution imaging at the Magellan 6.5 m telescope with the MIRAC/BLINC camera. We detected emission from a compact region surrounding the nuclear source and obtained photometry at 8.8 μm and in the N band. Our analysis suggests that the nuclear region is resolved with a size of ≈ 3 pc. The mid-IR emission from this region is likely associated with cool dust with an estimated temperature of ~ 160 K, surrounding the central “hidden” active galactic nucleus (AGN). We discuss the characteristics of this emission in relation to other mid-IR observations and the implications on models of dust formation in AGNs.

Subject headings: galaxies: active — galaxies: individual (Centaurus A, NGC 5128) — galaxies: nuclei — techniques: high angular resolution

1. INTRODUCTION

The nearest radio-bright active galactic nucleus (AGN) is located at a distance of “only” ~ 3.5 Mpc in the giant elliptical galaxy NGC 5128 (Cen A; *vis review* by Israel 1998). The central engine powering this galaxy is thought to be a super-massive black hole enshrouded in a region containing dust and gas heated by the central source (Marconi et al. 2001). Multi-wavelength observations of Cen A reveal many complex multi-scale structures, at scales ranging from a subparsec to hundreds of kiloparsecs (e.g., Karovska et al. 2002). A radio and X-ray jet powered by the central source extends across the galaxy to a distance of several hundreds of kiloparsecs from the nucleus. Optical and near-IR images of Cen A show large spatial scale (several kiloparsecs in size) dark bands stretching across the middle of the galaxy and obscuring the central region, probably because of absorption by dust and other cool material. These dust lanes are thought to be a remnant of a merger with a smaller spiral galaxy (Schiminovich et al. 1994). Using mid-infrared and submillimeter wavelength observations of the central region of Cen A, Mirabel et al. (1999) detected dust emission from a large-scale bisymmetric structure (5 kpc in size) resembling a barred spiral galaxy.

Because of its proximity, Cen A provides a unique possibility for high spatial resolution studies of the circumnuclear environment of AGNs using ground- and space-based large-aperture telescopes ($0''.1$ corresponds to ~ 1.5 pc at the Cen A distance of ~ 3.5 Mpc). However, exploring the nuclear region of Cen A at optical wavelengths presents a major challenge because of the high extinction (e.g., $A_V \sim 10$ mag; Alexander et al. 1999) due to heavy obscuration by the dust in the dust lanes.

Although the diffraction-limited telescope resolution is significantly lower in the mid-IR when compared to the optical (~ 10 times), the spectral range from 8 to 20 μm is, nevertheless, particularly suitable for studying the emission from the region surrounding the nucleus because of at least 10 times lower opacity. The lower opacity of astronomical dust at these wavelengths (Draine & Lee 1984) permits penetration of the optically opaque dust lanes. Most of the thermal radiation from dust is in fact emitted at these wavelengths, as seen in the mid-IR ISOCAM spectra of Cen A, which show the presence of

the characteristic silicate broad absorption feature at 9.8 μm , plus a possible polycyclic aromatic hydrocarbon (PAH) emission line at 11.3 μm . Alexander et al. (1999) suggested that the presence of a very deep 10 μm silicate absorption feature in the ISOCAM spectrum could be due to self-absorption in a dusty circumnuclear region, in addition to the extinction by the dust in the dust lanes (optical depth $\tau_v \approx 1$ at 10 μm).

We report here results from our mid-IR imaging of Cen A with the Mid-InfraRed Array Camera/Bracewell Infrared Nulling Cryostat (MIRAC/BLINC) at Magellan, showing that the nuclear region is resolved at a subarcsecond scale. The observations and the techniques for data acquisition and reduction are described in the next section. Results and analysis are presented in § 3 and discussed in relation to other available observations and models in § 4.

2. OBSERVATIONS AND DATA REDUCTION

During an exploratory observation of Cen A on 2002 May 1 and 2 at the Magellan I (Baade) telescope, we detected a compact mid-IR source in the images of the nuclear region at 8.8 μm and in the N band. The Baade telescope, with a primary aperture of 6.5 m equipped with active optics, provides diffraction-limited subarcsecond images in the 8.8 μm spectral window (Shectman & Johns 2003). The images of Cen A and several reference sources were recorded using MIRAC/BLINC. MIRAC/BLINC uses a Boeing HF16 128 \times 128 Si:As blocked impurity band detector (Hoffmann et al. 1998).

We obtained images using the MIRAC/BLINC 8.8 μm 10% passband filter and the wide N -band filter (from 8.1 to 13.1 μm) centered at 10.3 μm . The total on-source integration time was 1400 s at 8.8 μm and 900 s in the N band. The reference stars γ Cru and IRC +10220, observed while transiting at a similar air mass as the source, provide flux and point-spread function (PSF) calibration information. To insure similar observing conditions, including similar telescope orientation, air mass, and seeing conditions, the observations of Cen A were made close in time (within a couple of hours) to the observations of the corresponding reference stars. In addition, we used the Magellan telescope active optics (looking at standard stars in the field of view) to monitor the seeing stability, by checking that

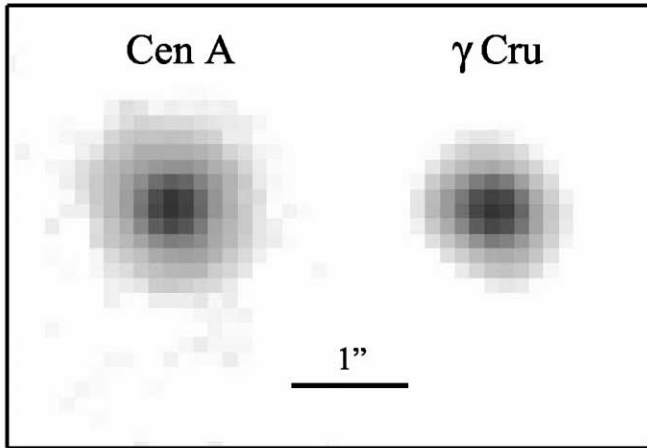


FIG. 1.—MIRAC/BLINC images of Cen A (*left*) and the reference star γ Cru (*right*) at $8.8 \mu\text{m}$. North is rotated 126° to the left (from the vertical).

the size and shape of the PSF at the beginning of each observation of Cen A is consistent with those of the corresponding reference.

On the Magellan, MIRAC/BLINC has a plate scale of $0''.12 \text{ pixel}^{-1}$, providing a total field of view of $17'' \times 17''$. This pixel scale ensures Nyquist sampling of the diffraction-limited PSF. As described below, we obtained further subsampling of the PSF by using dithering techniques. We used a standard nodding and chopping technique to remove the background signal, dithering the source on the array to obtain subsampling of the PSF. Chopping is carried out through rotation of an internal mirror to mitigate noise due to sky brightness fluctuations. The chop frequency was set to 10 Hz, with a throw of $8''$ in the north-south direction. The nod throw was also set to $8''$, but in the east-west direction, in order to have all four chop-nod beams inside the field of view of the array. Each individual nod cycle required 15 s ($8.8 \mu\text{m}$) or 10 s (N band) on-source integration, and the procedure was repeated for as many cycles as needed to obtain the total integration time at each wavelength.

The data were analyzed by first subtracting the chop-on from the chop-off frames for both nodding beams. The two images thus obtained were then subtracted one from the other, in order to get a single frame in which the source appears in all four beams (two negative and two positive). We then applied a gain matrix, derived from images of the dome (high-intensity uniform background) and the sky (low-intensity uniform background), to flat-field the chop-nodded image. This procedure was repeated for each of the nodding cycles for which the source was observed. A final high signal-to-noise ratio (S/N) cumulative image was then obtained by co-adding together all the beam frames, each recentered and shifted on the source centroid. This last co-adding step was performed on a subpixel grid, providing a final pixel scale of $0''.03 \text{ pixel}^{-1}$. A mask file to block out the effects of bad pixels and field vignetting was also created and applied at each individual frame before their shifting, preventing individual rejected pixels from contributing to the final image. To ensure a uniform treatment of the source and the standard, the same observing and reduction procedure was also used for the reference star.

3. RESULTS AND ANALYSIS

3.1. Imaging of the Circumnuclear Region

The mid-IR images of the nuclear region of Cen A obtained at $8.8 \mu\text{m}$ and in the N band are systematically larger than the

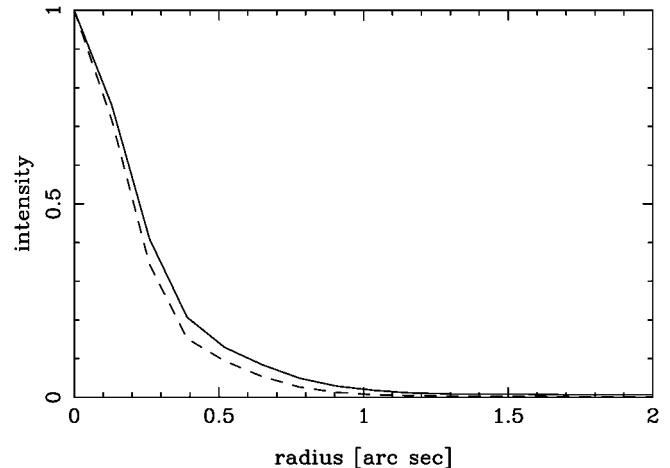


FIG. 2.—Radial profiles of Cen A image (*solid line*) and of the reference image (*dashed line*) at $8.8 \mu\text{m}$. The radial profile of Cen A appears more extended when compared to the radial profile of the reference star, indicating therefore that Cen A is resolved.

unresolved reference sources (or the “observed” PSFs) recorded under similar observing conditions and using the same filters. In Figure 1 we show the images of Cen A and the reference star γ Cru obtained at $8.8 \mu\text{m}$. The comparison of image sizes clearly shows that the Cen A image of the nuclear region is larger than the image of the unresolved pointlike reference source at this wavelength. We note that the $8.8 \mu\text{m}$ images of Cen A and the reference have better resolution and are of higher S/N than the images obtained in the wide N band centered at $10 \mu\text{m}$.

The difference in size between the point source and the Cen A nuclear region is shown in Figure 2, which displays the radial profiles of the source and the reference at $8.8 \mu\text{m}$ normalized at the same peak value. This suggests that the Cen A nuclear region is resolved, with the size near the resolution limit of the Magellan 6.5 m telescope. We estimated the angular size of the Cen A nuclear region by convolving the reference star radial profile with a Gaussian and then fitting to the Cen A data at the corresponding bandpasses. The best fit at $8.8 \mu\text{m}$ gives a FWHM of $0''.17 \pm 0''.02$. The N -band size estimate is consistent, with larger error bars because of the lower S/N in these data.

At the distance of Cen A, the measured FWHM angular size corresponds to a linear size of $\approx 3 \text{ pc}$, or $\sim 10 \text{ lt-yr}$. This is in agreement with the predicted size of the dust-emitting region based on model fitting of ISOCAM spectra with emission from the dust lanes and from a separate toroidal dust region around the nucleus with a diameter of $\sim 3.6 \text{ pc}$ (Alexander et al. 1999).

3.2. Photometry

We obtained photometry of the nuclear region using Cen A images in the two observed bandpasses by selecting a small aperture centered on the nuclear region. We used an aperture with a diameter of 20 MIRAC/BLINC pixels, corresponding to $\sim 2''.4$, which is the minimum aperture size that includes most of the PSF flux. The photometric reference for the $8.8 \mu\text{m}$ image was γ Cru, which has a known flux of 1090 Jy at that wavelength, with an estimated uncertainty of 5% (Gezari, Schmitz, & Mead 1987, p. 1196). For the N band we used the source IRC +10220 as a reference. We estimated for this star an N -band magnitude of $\sim 1.5 \text{ Jy}$, with a 30% uncertainty, based on interpolation of the K magnitude of 2.84 ($\sim 45 \text{ Jy}$) and the IRAS $12 \mu\text{m}$ flux of $\sim 4 \text{ Jy}$ from Gezari et al. (1987) (Table 1).

The photometry of the Cen A nuclear region was calculated

TABLE 1
MID-IR PHOTOMETRY

Source	Wavelength (μm)	Photometry (Jy)
Cen A	8.8	0.9 (± 0.1)
	10.3	1.4 (± 0.5)
γ Crux	8.8	1009 (± 50)
IRC +10220	10.3	1.5 (± 0.4)

separately for the four nod/chop beams at each wavelength, which were then averaged together. This procedure ensured that the variation in the photometry of the four beams was within our error estimate. We also evaluated different sizes of the aperture and of the sky region for residual background subtraction, from $1''.5$ to $5''$, finding similar values of the photometry, within our error bars ($\pm 1 \sigma$). We obtained an average flux of 0.9 Jy at $8.8 \mu\text{m}$, with an uncertainty of ± 0.1 Jy, and a flux of 1.4 Jy in the N band, with an uncertainty of ± 0.5 Jy (Table 1). The significant uncertainties are due to the limited photometric quality of the sky during these observations. Larger aperture photometry (several arcseconds aperture) does not show significant differences within the error bars with the smaller aperture results that we are presenting in this Letter.

Our photometric results are in agreement with the mid-IR observations obtained by Whyson & Antonucci (2002) using the Keck I telescope. They detected emission from a compact unresolved nuclear source (with an upper limit on the size of $\sim 0''.3$) and measured fluxes of 1.6 and 2.3 Jy at 11.7 and $17.75 \mu\text{m}$, respectively.

Our results are also in agreement within $\approx 3 \sigma$ errors with the ISOCAM circular variable filter (CVF) spectrum obtained by Mirabel et al. (1999), which gives ~ 0.7 Jy at $8.8 \mu\text{m}$. In Figure 3, we plot our photometric results on the ISOCAM CVF spectrum (see Fig. 2 in Mirabel et al. 1999). The spectrum shows a broad silicate absorption feature around $9.8 \mu\text{m}$, resulting in a lower flux at $10.3 \mu\text{m}$ with respect to $8.8 \mu\text{m}$.

Given the limited photometric and spectral accuracy of our mid-IR data, we cannot discriminate between thermal emission from dust and the emission from late-type stars photospheres, because we essentially have only one color (the $8.8 \mu\text{m}$ filter is inside the N filter wave band). It is also likely that the eventual stellar radiation in the nuclear region is below our sensitivity limit. We therefore assume that the emission in the circumnuclear region is thermal, originating from dust surrounding the inner hot region.

3.3. Dust Temperature

Using the estimated size of the circumnuclear region at $8.8 \mu\text{m}$ and the flux measurements based on our mid-IR observations, we derive an estimate of the temperature of the emitting dust. We assume that the emission is a blackbody thermal emission and that there is an absorbing component associated with the dust lanes in front of the central source. For a simple spherical geometry of the emitting region, we estimate the dust temperature at $8.8 \mu\text{m}$ using the following expression derived from the Planck law:

$$T = 1440 \left[\ln \left(1 + 1.1 \times 10^5 \frac{R^2 e^{-\tau_\nu}}{D^2 F_\nu} \right) \right]^{-1}, \quad (1)$$

where T is the dust temperature in kelvins, R is the radius of the region in parsecs, F_ν is the flux in janskys, and τ_ν is the optical depth of the dust lanes.

Using a radius of ≈ 1.5 pc for the circumnuclear dust region,

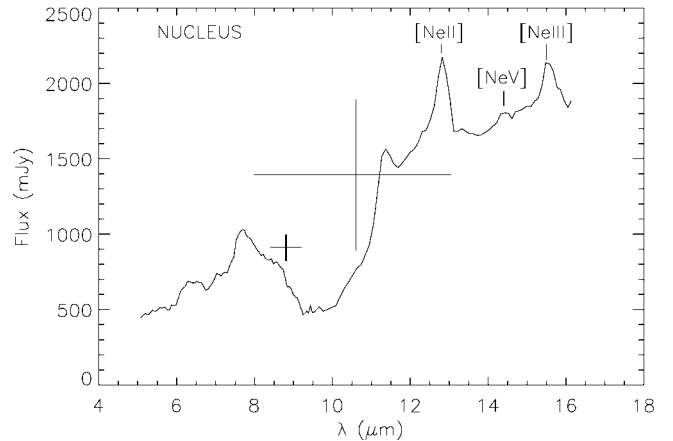


Fig. 3.—ISOCAM CVF spectrum of the nuclear region ($4''$ radius) of Cen A (Mirabel et al. 1999) showing several emission lines and a deep silicate absorption feature at $\sim 9 \mu\text{m}$. Also plotted are the results from our $8.8 \mu\text{m}$ and N -band photometry of the $2''.4$ region centered on the nucleus.

flux of 0.9 Jy, and $\tau_\nu \sim 1$ for the dust lane's optical depth at $\sim 10 \mu\text{m}$, we estimate the dust temperature at ≈ 160 K. We compare the temperature obtained using this simplified model with the temperature derived from the ISOCAM spectra. The multicomponent spectral fit (see Fig. 3 in Alexander et al. 1999) shows that the mid-IR emission from the circumnuclear region peaks at $20 \mu\text{m}$, which corresponds to a dust temperature of $T \approx 150$ K. This is in agreement with the estimated dust temperature of the circumnuclear region based on our mid-IR measurements.

4. CONCLUSIONS

The results of our mid-IR imaging and photometry of the Cen A nuclear region suggest that the emission originates from a resolved source ≈ 3 pc in diameter. This emission is likely to be thermal radiation from dust at ≈ 150 K heated by UV/optical radiation from a “hidden” central AGN source (e.g., Peterson 1997; Whyson & Antonucci 2002). It is possible that we are detecting the external cooler region, possibly surrounding hotter inner dust ($T \sim 1000$ K), as suggested by the deep silicate absorption feature in the *Infrared Space Observatory* spectra around $10 \mu\text{m}$.

Resolving the source of mid-IR emission in the nuclear region of Cen A provides an important key for understanding dust formation processes and the structure of the nuclear region of AGNs and quasars. For example, the current “unified” model of AGNs predicts a dusty torus with a size of ~ 10 lt-yr surrounding the accretion disk and a black hole central engine (Antonucci & Miller 1985; Krolik & Begelman 1988; Peterson 1997). The predicted size of the torus is of the order of the measured size of the Cen A circumnuclear region using our mid-IR imaging. We note that the estimated size of the Cen A circumnuclear region is also similar to the size of the dusty region (~ 3 pc) surrounding the central source of NGC 1068, recently resolved AGN using the Very Large Telescope Interferometer observations (ESA Press release 17/03).

The measured size of the mid-IR-emitting region is also comparable to the distance from the central source at which dust will condense in an outflowing AGN wind. As recently demonstrated by Elvis, Marengo, & Karovska (2002), dust can be created from cooling broad emission line clouds in AGN winds and can survive in the quasar environment because of self-shielding. This implies that Cen A could effectively be

recycling dust from the host galaxy interstellar medium into the intergalactic medium while changing the dust size and distribution and the dust-to-gas ratio. The possibility that AGNs or quasars can provide an additional path for dust formation has important cosmological implications, since it could explain in a natural way the observed heavy obscuration of distant quasars (Omont et al. 2001; Elvis et al. 2002) and provide a new means of forming dust at early cosmological times.

The current observations do not have enough accuracy to determine the true geometry of the emitting region or to distinguish between different geometries suggested by AGN models. The observations were challenging because of the limited telescope resolution. Further multiwavelength observations of Cen A with higher spatial resolution are crucial to explore the geometry of the extended nuclear region and derive the physical characteristics and the origin of the emission. Multiband mid-IR observations combined with spectroscopy will allow deter-

mination of the characteristics of the circumnuclear dust, including its temperature, and an estimate of the mass and mass loss rate. The results may further constrain the unified AGN model and models of dust formation in quasar outflows.

We thank the Magellan staff for their outstanding support. We are grateful to Scott Wolk for valuable suggestions and aid in preparing the manuscript, to Felix Mirabel for allowing us to use the ISOCAM CVF spectrum, and to the anonymous referee for useful comments and suggestions. M. K. and M. E. are members of the *Chandra* X-ray Center, which is operated by the Smithsonian Astrophysical Observatory under contract to NASA NAS8-39073. This research was supported in part by NASA through the American Astronomical Society's Small Research Grant Program. MIRAC is supported through SAO and NSF grant AST 96-18850. BLINC is supported through the NASA Navigator program.

REFERENCES

- Alexander, D. M., Efstathiou, A., Hough, J. H., Aitken, D., Lutz, D., Roche, P., & Sturm, E. 1999, *MNRAS*, 310, 78
 Antonucci, R. R. J., & Miller, J. S. 1985, *ApJ*, 297, 621
 Draine, B. T., & Lee, H. M. 1984, *ApJ*, 285, 89
 Elvis, M., Marengo, M., & Karovska, M. 2002, *ApJ*, 567, L107
 Gezari, D. Y., Schmitz, M., & Mead, J. M. 1987, *Catalog of Infrared Observations, Part I* (Washington, DC: NASA)
 Hoffmann, W. F., Hora, J. L., Fazio, G. G., Deutsch, L. K., & Dayal, A. 1998, *Proc. SPIE*, 3354, 647
 Israel, F. P. 1998, *A&A Rev.*, 8, 237
 Karovska, M., et al. 2002, *ApJ*, 577, 114
 Krolik, J. H., & Begelman, M. C. 1988, *ApJ*, 329, 702
 Marconi, A., Capetti, A., Axon, D. J., Koekemoer, A., Macchetto, D., & Schreier, E. J. 2001, *ApJ*, 549, 915
 Mirabel, I. F., et al. 1999, *A&A*, 341, 667
 Omont, A., et al. 2001, *A&A*, 374, 371
 Peterson, B. 1997, *An Introduction to Active Galactic Nuclei* (Cambridge: Cambridge Univ. Press)
 Schiminovich, D., van Gorkom, J. H., van der Hulst, J. M., & Kasow, S. 1994, *ApJ*, 423, L101
 Sheckman, S., & Johns, M. 2003, *Proc. SPIE*, 4837, 910
 Whyson, D., & Antonucci, R. 2002, preprint (astro-ph/0207385)